ORIGINAL PAPER

Assessment of Dynamic Behaviour and Performance of Existing Composite Railway Bridges Under the Impact of a High-Speed LHB Train Using a Coupled Approach

Naveen Kumar Kedia[1] · Anil Kumar[2] · Yogendra Singh[3]

Abstract

Purpose The current study focuses on the dynamic behaviour and performance of existing steel-concrete composite bridges subjected to high-speed LHB trains. The research focuses on the dynamic behaviour of the bridge structure, taking into account natural frequency, resonance characteristics, acceleration, displacement, and dynamic impact factor. Sperling's ride index is used to assess the train's dynamic performance passing across bridges. The environmental effect of the train-track-bridge system is also evaluated following ISO 2631 recommendations.

Methods Each vehicle is represented using multibody dynamics having 10 degrees of freedom. The bridge and track structure is modelled as an Euler beam divided into several elements of equal lengths with continuous elastic support between them. The train and track-bridge subsystems are modelled as a coupled system that interacts through the wheel-rail interaction forces. The study is being conducted for three separate Indian Railways bridges with span lengths of 19.4 m, 25.28 m, and 31.9 m. The analysis utilises the characteristics of a ballasted track structure with soft to stiff rail pads.

Results and Conclusions It is found that a train at a higher speed can operate safely on the existing bridges. However, the dynamic behaviour of a bridge at resonance is critical for all the span lengths, exceeding the bridge impact factor limits set by various national and international standards such as AASTHO, RDSO and AREMA. The environmental concern of high speed trains is also prevalent as vibration level exceeds the limit set by FTA for various land use categories. The effect of track properties on the bridge response is not much visible; however, Sperling's ride comfort index varied considerably and surpassed the threshold value of 2.5 for the span length of 25.28 m and 31.9 m at higher speeds.

Keywords Finite element method · Railway bridge · Ride comfort · Environmental vibration · High-speed train

Introduction

Railway transportation is one of the fastest-growing modes of transportation for both inter and intra-city movements. The rise in metro facilities, monorail, tram services and high-speed trains globally is clearly at par with the recent technological advancements in railway engineering. Most developing economies such as India, Brazil [1], Turkey, and Saudi Arabia, are developing new high-speed corridors. At the same time, they want to exploit the maximum capacity of their existing massive rail infrastructures comprising railway tracks, trains, stations and bridges. Indian Railways is no exception and is currently focused on updating its existing infrastructure, increasing the speed of the current passenger and freight trains and introducing new high-speed corridors [2]. Simultaneously, the Indian Railways is working to utilise the existing bridge and track

✉ Anil Kumar
  anil.kumar@me.iitr.ac.in

  Naveen Kumar Kedia
  nkedia@ct.iitr.ac.in

  Yogendra Singh
  yogendra.singh@eq.iitr.ac.in

1 Centre for Transportation Systems, Indian Institute of Technology Roorkee, Roorkee 247667, India

2 Department of Mechanical and Industrial Engineering, Indian Institute of Technology Roorkee, Roorkee 247667, India

3 Department of Earthquake Engineering, Indian Institute of Technology Roorkee, Roorkee 247667, India

capacity to run the train at a higher speed. As a result, it is critical to investigate the impact of high-speed trains on existing infrastructure. Railway bridges are an essential element of the railway infrastructure, and it is crucial to examine the impact of high-speed trains on bridge dynamics and performance [3]. The current study focuses on the train–track–bridge interaction [4] of a composite steel–concrete bridge in the context of, but not limited to, Indian Railways. The emphasis is on examining the dynamic behaviour of existing bridge structures under the effect of high-speed trains, evaluating the train's safety in terms of ride comfort, and analysing the high-speed train's environmental impact on the nearby structures and human settlements.

The study of railway dynamics is a subject of great interest and is still being explored due to the complexities in train–bridge interaction behaviour [5]. The high-speed train produces a considerable vibration on the bridge structure, which affects the bridge's serviceability and is also a concern for train vehicle safety, reducing passenger ride comfort [6]. The steel–concrete composite bridges are used extensively for the high-speed railway network in developed countries such as Japan, China, and European nations due to significant advantages related to the structure's design, durability, and cost. However, it is necessary to check and evaluate the problems associated with dynamic effects and interaction phenomenon, fatigue loading, structural modelling and damage assessment [7]. The bridge resonance, in particular, is among various response characteristics that is of interest mainly due to the structural safety of the bridge [8, 9]. Due to their lightness and damping capacities, composite bridges can experience resonance-induced vibration at speeds slower than the design speed [10].

Liu et al. [11] studied the fatigue assessment of the composite Sesia viaduct and identified train speed and mass ratio as significant factors that determine the dynamic effect. Adam et al. [12] analysed the dynamic response of compound bridges under moving loads. Nguyen et al. [13] presented the analytical models for dynamic analysis of short skew bridges under moving loads and found that the degree of skewness has an important influence on the vertical displacement but hardly on the vertical acceleration of the bridge. Hoorpah [14] studied the dynamic analysis of high-speed railway composite bridges in France. Sieffert et al. [15] studied the application of a diaphragm at midspan on the static and dynamic behaviour of a composite railway bridge and concluded that a diaphragm is not necessary except for accidental lateral loads. Melo et al. [16] performed the train-bridge system's dynamic analysis, considering the non-linear behaviour of the track–deck interface. Matsuoka et al. [17] focused on the dynamic simulation and critical assessment of a composite bridge in a high-speed railway for a case study of the Sesia viaduct. Shibeshi and

Roth [18] conducted a dynamic analysis of a 77-year-old single-span steel truss railway bridge using experimental, analytical and three-dimensional finite element analysis.

The periodic loading due to moving train gives rise to the driving and dominant frequencies. When these frequencies or their integral multiples match the fundamental frequency of the bridge, there is amplification in the bridge's global response [19, 20], which might affect the bridge's and train's serviceability [21, 22]. The passenger ride comfort can decrease substantially due to amplification in the bridge response. Ride comfort depends on several factors such as bridge span length, train speed, train compartment length, vehicle suspension, etc. [23–25]. Ride comfort can be measured using Sperling's ride index based on the Wz method (Werzungzahl) [26], ISO 2631 standard [27] and the European method [28].

The environmental impact of high-speed trains is another critical area that needs attention. The effect of high-speed trains is always portrayed as an environment-friendly mode of transportation [29]. However, high-frequency noise and low-frequency vibration originating at the wheel–rail interface interfere with equipment working, affect the structure's durability [30, 31] close to the rail track and causes a nuisance in the nearby facilities [32–34] demanding the application of suitable mitigation measures [35]. The Federal Transit Administration [36] (FTA) has issued guidelines to limit the intensity of train-induced vibrations. The methods for controlling train-induced vibration are divided into three stages: generation, propagation, and reception. The primary approach is to dampen the vibrations at the source, and the track structure's elastic support absorbs the energy transmitted owing to ground vibration propagation [37]. Proper vibration assessment in train–track–bridge interactions requires an accurate description of track structures. The modelling of layered track structure requires complex iterative models [38, 39]; however, analysis can be simplified using simple viscoelastic foundations [40].

Further, an efficient and accurate numerical model for the vehicle is necessary to model the load transfer between train and track [41]. The interaction between train and bridge is basically divided into three categories based on the modelling strategy adopted, i.e. moving load, moving mass and moving spring-damper system model. The moving load model [42] is the simplest and most efficient but cannot consider the train–bridge interaction effect, which can be studied using the moving mass model [43]. The moving mass spring damper system [44, 45] combines lumped masses, rigid bars, and spring and dashpot, considering interaction and vehicle motion.

In the comprehensive discussion above, it is clear that bridge dynamics has been a topic of interest from the early days, and continuous research in this field is necessary with the advancement in railway technology. The

two-dimensional (2D) finite element method (FEM) [46, 47] is used to develop the train–track–bridge interaction model with the application of the coupled approach [48]. The moving mass-spring-damper system is used for vehicle modelling. The properties of Linke Hofmann Busch (LHB) trains and composite steel–concrete railway bridges of Indian Railways are used for parametric studies. The modelling strategy adopted is discussed in Sect. 2, and validation of the numerical model is shown in Sect. 3. The ride comfort is discussed in Sect. 4, and parametric analysis is performed in Sect. 5. Finally, the significant outcomes are discussed in Sect. 6.

The Train–Track–Bridge Dynamic Interaction Model

The dynamic interaction model is developed using the 2D FEM and solved using numerical techniques based on the dynamic interaction one proposed by Zhai and Cai [49]. The analysis is bifurcated into two separate subsystems, i.e. vehicle and track–bridge. The interaction between the two subsystems is accomplished by the wheel–rail interaction forces that arise at the interface [41].

Train System

The properties of the LHB air-conditioned (AC) two-tier German-designed broad gauge (BG) coach with a seating capacity of 48 [50, 51] is used to assess the ride comfort and evaluate the dynamic response of a bridge at critical locations. The multibody dynamics concept [52, 53] is used to model a train where a vehicle's degrees of freedom (DOFs) are assigned to the vehicle's body's motion. The train running on the bridge at a constant speed combines several carriages and locomotives. Figure 1 illustrates a train's numerical model where each component, i.e. carbody, bogie and wheelset, is modelled as a rigid body
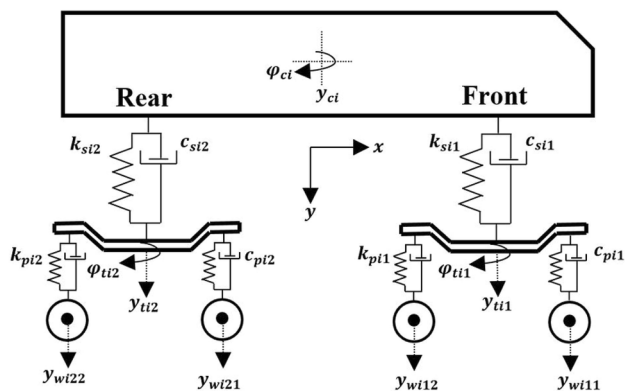

Fig. 1 10 DOFs 4-axle vehicle model

connected by spring and damper elements. Each carbody and bogies have vertical and pitch displacement, and for each wheelset, only vertical displacement is considered. Thus, a total of 10 DOFs is established for a 4-axle train vehicle. Here, y_{ci} is the vertical displacement of an ith carbody ($i = 1 - 10$); y_{tij} is the vertical displacement of jth bogie of an ith carbody ($j = 1 - 2$); φ_{ci} is the pitch displacement of an ith carbody; φ_{tij} is the pitch displacement of jth bogie of an ith carbody; y_{wijl} is the vertical displacement of lth wheelset of jth bogie of an ith carbody ($l = 1 - 4$).

However, the vertical displacement of the wheelset is restrained by the rail displacement, reducing the vehicle-independent DOFs to six. The 10 LHB coaches are considered in the present work, and their technical specifications are shown in Table 1. The mass matrix M_v of a vehicle with the order $\left(6 \times N_v\right) \times \left(6 \times N_v\right)$ is written as follows;

$$M_v = \text{diag}\left[M_{v1}\ M_{v2}\ \cdots\ M_{v10} \right], \tag{1}$$

here M_{vi} is a mass matrix of an ith vehicle and can be written as follows;

$$M_{vi} = \text{diag}\left[m_c\ j_c\ m_{br}\ j_{br}\ m_{bf}\ j_{bf} \right], \tag{2}$$

here subscripts r and f represent the rear and front bogie.

The stiffness matrix K_v of a vehicle with the order $\left(6 \times N_v\right) \times \left(6 \times N_v\right)$ is written as follows;

$$K_v = \text{diag}\left[K_{v1}\ K_{v2}\ \cdots\ K_{v10} \right], \tag{3}$$

here K_{vi} is a stiffness matrix of an ith vehicle and can be written as follows;

Table 1 Technical specifications of LHB coaches [50, 51]

S. no	Parameters	Value
1	Carbody mass $\left(m_c\right)$	46,720 kg
2	Bogie mass $\left(m_b\right)$	6300 kg
3	Wheelset mass $\left(m_w\right)$	1600 kg
4	Primary stiffness $\left(k_p\right)$	11.06×10^5 N/m
5	Secondary stiffness $\left(k_s\right)$	6.12×10^5 N/m
6	Primary damping $\left(c_p\right)$	32,600 N s/m
7	Secondary damping $\left(c_s\right)$	40,200 N s/m
8	Rotational inertia of carbody $\left(j_c\right)$	56,932 kg/m^2
9	Rotational inertia of bogie $\left(j_b\right)$	1732 kg/m^2
10	Bogie axle base $\left(2L_b\right)$	2.56 m
11	Hoz. distance b/w the C.O.G of carbody and rear bogie $\left(L_1\right)$	7.45 m
12	Hoz. distance b/w the C.O.G of carbody and front bogie $\left(L_2\right)$	7.45 m
13	Interbogie spacing	6.54 m
14	No. of vehicles $\left(N_v\right)$	10

$$K_{v1} = \begin{bmatrix} 2k_s & -k_sL_1 + k_sL_2 & -k_s & 0 & -k_s & 0 \\ -k_sL_1 + k_sL_2 & k_sL_1^2 + k_sL_2^2 & k_sL_1 & 0 & -k_sL_2 & 0 \\ -k_s & k_sL_1 & k_s + 2k_p & 0 & 0 & 0 \\ 0 & 0 & 0 & 2k_pL_b^2 & 0 & 0 \\ -k_s & -k_sL_2 & 0 & 0 & k_s + 2k_p & 0 \\ 0 & 0 & 0 & 0 & 0 & 2k_pL_b^2 \end{bmatrix}. \quad (4)$$

The damping matrix C_v of a vehicle with the order $(6 \times N_v) \times (6 \times N_v)$ is written as follows;

$$C_v = \text{diag}\begin{bmatrix} C_{v1} & C_{v2} & \cdots & C_{v10} \end{bmatrix}, \quad (5)$$

here C_{vi} is a stiffness matrix of an ith vehicle and can be written as follows;

Fig. 2 Ballasted track system

$$C_{v1} = \begin{bmatrix} 2c_s & -c_sL_1 + c_sL_2 & -c_s & 0 & -c_s & 0 \\ -c_sL_1 + c_sL_2 & c_sL_1^2 + c_sL_2^2 & c_sL_1 & 0 & -c_sL_2 & 0 \\ -c_s & c_sL_1 & c_s + 2c_p & 0 & 0 & 0 \\ 0 & 0 & 0 & 2c_pL_b^2 & 0 & 0 \\ -c_s & -c_sL_2 & 0 & 0 & c_s + 2c_p & 0 \\ 0 & 0 & 0 & 0 & 0 & 2c_pL_b^2 \end{bmatrix}. \quad (6)$$

The use of a 2D train numerical model is only suitable to study the vertical vibrations, and the lateral dynamics is neglected, in the present study. The use of 2D analysis is motivated by the assumption that the vertical bridge vibration will primarily affect the vertical response of the vehicle. Moreover, the comparison of 2D and 3D vehicle models carried out by Arvidsson et al. [25] shows an excellent agreement of the wheel–rail force between the 2D and 3D models.

Bridge Systems

The present analysis uses composite girder railway bridges designed for a 25t loading of three different span lengths. The ballasted track system shown in Fig. 2 is primarily used by the Indian railways for surface and elevated corridors. The track system consists of rail, rail pads, sleepers, and ballast. In a dynamic coupled analysis, the track is crucial because it transfers load from the wheels to the bridge deck and reduces vibration. The schematic layout of a simply supported composite railway bridge is shown in Fig. 3a and b. It consists of two—I shape riveted steel girders, horizontal
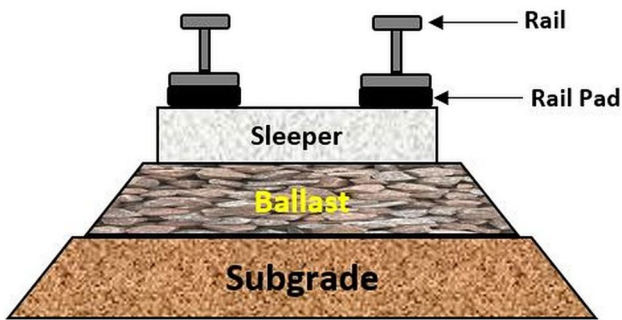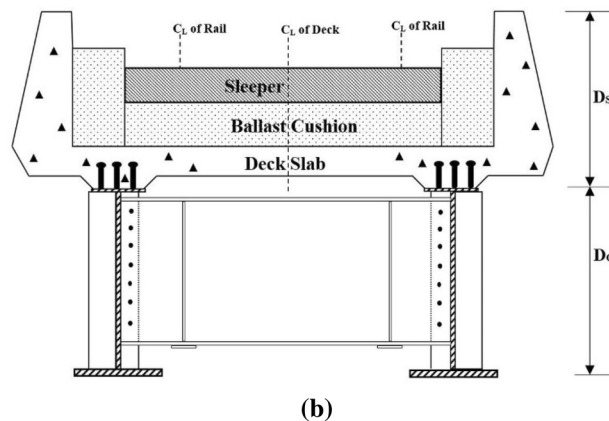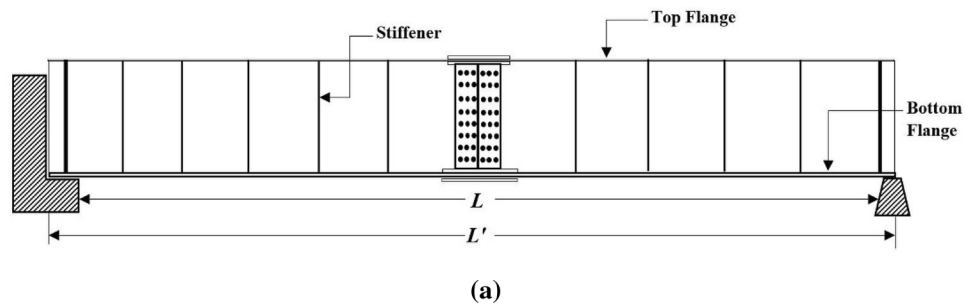
Fig. 3 Schematic representation of a bridge. **a** Side view. **b** Cross-sectional view

(a)

(b)

and vertical brace systems, concrete deck slabs, sleepers and rail systems.

The concept of a 2D FEM is used to model track and bridge structures. Since the train–bridge interaction problem lies in an elastic range, a reduced model of a composite bridge is used to simplify an analysis in which steel girders are replaced with equivalent concrete structures using the modulus of elasticity. The fundamental behaviour of simply supported bridges can be described by the 2D Euler Bernoulli beams' dynamic behaviour [54–56]. Hence, the bridge structure is modelled as an Euler beam divided into several elements of equal lengths with elastic supports. The bridge's mass is assumed to be a cumulative mass of the bridge structure, and there is no vertical displacement in columns and foundations. Moreover, shear deformation is neglected and only bending is considered in a beam. These assumptions are equitable here as only the dynamic vibration of the bridge structure and vehicle dynamic behaviour are analysed. An embankment of equal length lies on the bridge's left and right side, and a rail is resting on a viscoelastic foundation for the entire length. The equivalent stiffness and damping of the viscoelastic foundation are calculated for soft to stiff pads using a spring analogy where rail pads, sleeper and ballast are considered in a series combination [57]. This simplification reduces the analysis's complexity and includes the effect of rail pads, sleeper, and ballast in the viscoelastic foundation. The bridge structures' global mass, stiffness and damping matrices are formulated using the classical 2D finite element theory discussed in several published literature [55, 58, 59].

It is to be noted here that, the use of 2D numerical model for the bridge neglects the torsional mode of vibrations in the bridge. However, this assumption holds good for the bridges having a torsional frequency much larger than the vertical vibration frequency. A 3D model of the considered bridges shows the ratio of torsional to vertical frequency as 5, which justifies the use of 2D model as per Eurocode EN 1990:2002 + A1 [60].

Train–Track–Bridge Coupling

The train and bridge subsystems are coupled together to form a dynamic coupled train–track–bridge interaction model. As shown in Fig. 4, the train moves at a constant speed on a

rail beam resting on a viscoelastic foundation. The embankment provided in a model ensures that the vehicle reaches a dynamic equilibrium before reaching a bridge [61].

The train–track–bridge coupled equations of motion solution are based upon time history integral techniques performed using numerical integration such as Newmark-β and Wilson-θ methods [62]. Xia. et al. [59] discussed three different methodologies for analysing train–bridge interaction problems, i.e. the direct coupling iteration method [63], in which equations of motion of various subsystems are established as a unified system. The in-time-step iteration method [64], where train and bridge systems are solved separately, and interaction is achieved through wheel–rail interaction forces. It is required that both the train and bridge systems fulfil the convergence requirement. The intersystem iteration method [65] is similar to the previous process; the only difference lies in convergence criteria. The wheel–rail interaction forces are used as an index for convergence judgment. Direct coupling is adopted in the present work to analyse the dynamic interaction between train, track and bridge. Each of the subsystems is defined by the second-order differential equation. The corresponding equation of a unified system in a submatrix form is represented by Eq. 7.

$$
\begin{bmatrix} M_v & 0 & 0 \\ 0 & M_T & 0 \\ 0 & 0 & M_B \end{bmatrix} \begin{Bmatrix} \ddot{X}_v \\ \ddot{X}_T \\ \ddot{X}_B \end{Bmatrix}
$$
$$
+ \begin{bmatrix} C_v & C_{VT} & 0 \\ C_{TV} & C_T & C_{TB} \\ 0 & C_{BT} & C_B \end{bmatrix} \begin{Bmatrix} \dot{X}_v \\ \dot{X}_T \\ \dot{X}_B \end{Bmatrix}
$$
$$
+ \begin{bmatrix} K_v & K_{VT} & 0 \\ K_{TV} & K_T & K_{TB} \\ 0 & K_{BT} & K_B \end{bmatrix} \begin{Bmatrix} X_v \\ X_T \\ X_B \end{Bmatrix} = \begin{Bmatrix} F_v \\ F_T \\ F_B \end{Bmatrix}
$$

(7)

Here, M, K, and C represent the global mass, stiffness and damping matrix of a system, together with the external force vector F solved for the X DOFs. The subscript v, T and B stand for a vehicle, track and bridge, respectively. The interaction between train and track is represented by matrices having subscript VT or TV and between track and bridge by
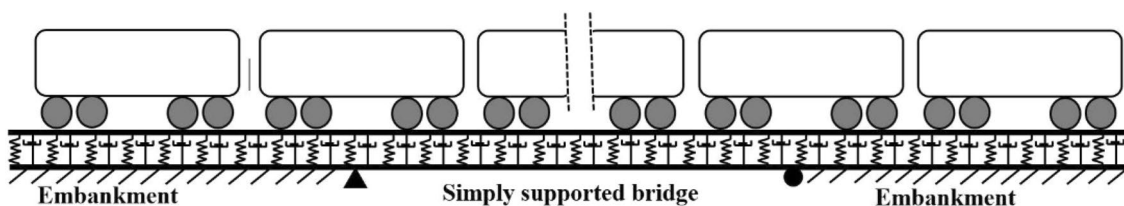

Fig. 4 Train–track–bridge coupled system

subscript *BT* or *TB*. The detailed derivation of these matrices can be found in papers [66, 67]. The coupling terms in Eq. (7) depend on the beam element's shape function and mechanical properties of the system. They are time-dependent terms, which means that their value must be updated at each time step of numerical integration. In the coupled approach, the DOFs of a wheel are integrated with the rail's DOFs. As a result, wheel masses are added to the track's mass matrix (M_T) at each time step [45]. The external force vector is the combined effect of gravity load and dynamic excitation due to the track profile at the wheel–rail interface [20, 68, 69]. The wheel–rail interaction forces are included in the formulation as an internal force in the coupled approach. The dynamic Eq. (7) is solved using the Newmark-β method to obtain the train, track and bridge responses. The damping in a bridge is defined using the Ryleigh Damping, in which the damping matrix is a linear combination of mass and stiffness matrix and is represented as follows;

$$C = \alpha[M] + \beta[K] \tag{8}$$

$$\alpha = \frac{2D\omega_1\omega_2}{\omega_1 + \omega_2} \text{ and } \beta = \frac{2D}{\omega_1 + \omega_2}, \tag{9}$$

here, ω_1 and ω_2 are the first and second circular natural frequencies of a bridge [70], and D is a damping ratio of 2% for the first and second bridge mode. The finite element model of rail and simply supported bridge is discretised in an element size of 0.5 m. The sensitivity analysis highlighted that a time step of 0.001 s gives a stable solution and is selected for numerical simulation.

Track Irregularity

The track irregularity profiles are generated using the power spectral density functions (Eq. 10) provided by the Federal Railroad Administration [71]. A sample profile of track irregularity along the track's longitudinal direction shown in Fig. 5 is generated using the trigonometric series or spectral representation method [55] for grades 1–6. The grade 6 track irregularity sample is used in the present work.

$$S_v(\omega) = KA\frac{\omega_c^2}{\left(\omega^2 + \omega_c^2\right)\omega^2}\left(\text{cm}^2/\text{rad/m}\right). \tag{10}$$

Validation of the Numerical Model

The numerical model is validated by the results published in the literature [67]. The analysis is done for a train running speed of 10–110 m/s with an increment of 2 m/s. The time
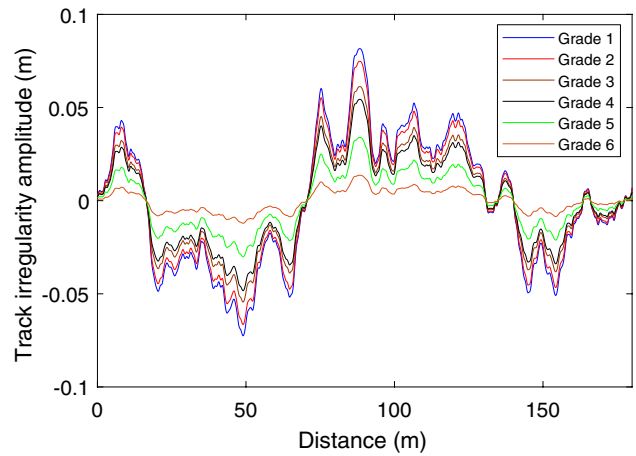

Fig. 5 Track irregularity

step of analysis is fixed to 0.0005 s for each speed, and train and track properties are taken from Ref. [67] (readers can refer to Tables 1 and 2 of Ref. [67] for train and track properties, respectively). Figure 6 compares the maximum value of bridge midpoint displacement and acceleration obtained from the numerical model with published work at various speeds. It can be seen that the numerical model is correctly predicting the outcome.

Ride Comfort

The train ride comfort is evaluated using Sperling's ride index (SI) [72], a well-known parameter in railway dynamics, to assess passengers' ride comfort. The SI is a low-cost computational technique compared to the other ride comfort indexes such as EN or UIC, which require a minimum of 5 min of acceleration time history. The stepwise methodology to evaluate SI is shown in Fig. 7.

The vertical car body acceleration is transformed to a frequency domain using the fast Fourier transform (FFT). Eventually, the Sperling frequency filter ($B(f)$) shown in Eq. (11) is applied to obtain the weighted car body acceleration in the frequency domain. The weighted acceleration in the time domain is acquired through inverse Fourier transform (IFT).

$$B(f) = \left\{0.588\left[\frac{1.911f^2 + \left(0.25f^2\right)^2}{\left(1 - 0.277f^2\right)^2 + \left(1.563f - 0.0368f^3\right)^2}\right]^{0.5}\right\}. \tag{11}$$

The SI (W_Z) is obtained using Eq. (12). Here, a_{rms} is the root mean square of the weighted acceleration in a time domain.

Fig. 6 Validation of the numerical model **a** comparison of maximum midpoint displacement, **b** comparison of maximum midpoint acceleration
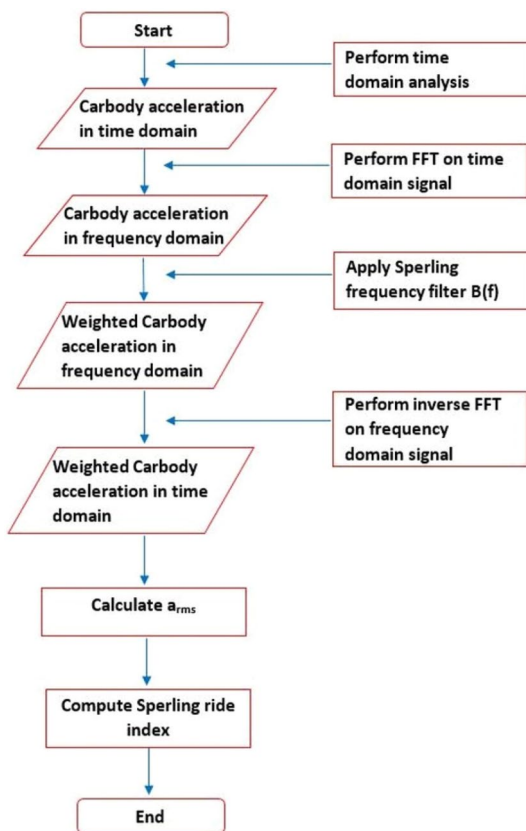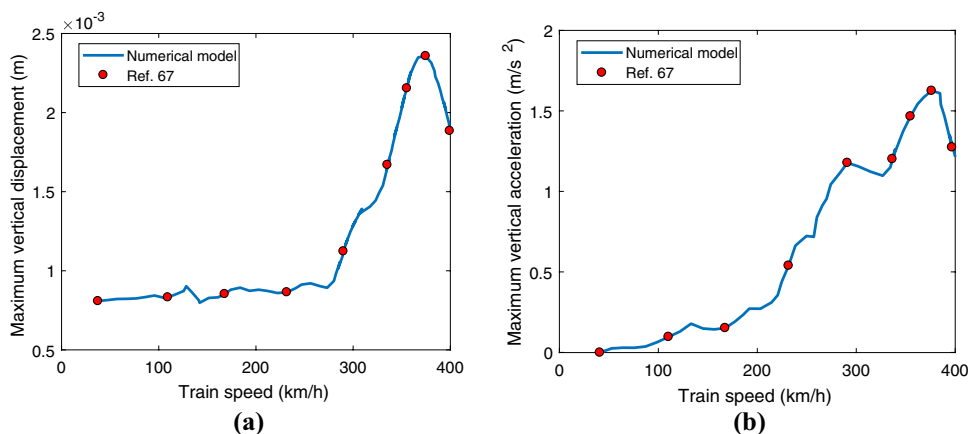

Fig. 7 Methodology to compute ride comfort index

Table 2 Ride comfort scales [73]

S. no	Wz	Ride comfort
1	1	Just noticeable
2	2	Clearly noticeable
3	2.5	More pronounced but not unpleasant
4	3	Strong, irregular, but still tolerable
5	3.25	Very irregular
6	3.5	Extremely irregular, unpleasant, annoying, prolonged exposure intolerable
7	4	Extremely unpleasant, prolonged exposure harmful

$$W_Z = 4.42 \left(a_{\mathrm{rms}} \right)^{0.3}. \quad (12)$$

The ride comfort conditions defined as per the range of SI are given in Table 2, and it is clear that for moderate and comfortable conditions, SI should be below 2.5.

The flexibility in a carbody is represented by an equivalent free-free Euler–Bernoulli beam, with a constant section and uniformly distributed mass to consider the

vertical bending modes. Several authors have used flexible models to evaluate the ride index. The literature review highlighted that for low and medium speed upto 250 km/h, not much difference is observed between the rigid and flexible car body models. However, for higher speed and low frequency of the first flexural mode, a significant difference is observed in ride index value for the rigid and flexible car body models. The study by Bokaeian et al. [74] highlighted the effect of bending flexural modes of the car body on the ride index. They concluded that the first bending flexural mode has the highest influence on the vehicle's ride quality. Moreover, the ride quality index is not affected significantly by flexural modes for the velocities between 140 and 250 km/h. However, for a train speed higher than 250 km/h, the effect of bending modes on the ride quality index becomes clear. The study by Kunpeng et al. [75] shows that car-body flexibility has little influence on bridge responses and vehicle running safety indices but greatly influences car-body accelerations. Dumitriu and Dihoru [76] showed that the contribution of the bending vibration is noticeable at high velocities, and at low bending vibration frequency difference is more vivid. Dumitriu and Cruceanu [77] highlighted the significance of the vertical symmetrical bending of the car body on the

vehicle's dynamic response, mainly at high velocities, and the ride comfort is greatly affected should the frequency of this vibration mode is lower than 10 Hz. Zhou et al. [78] concluded that at frequencies higher than 7 Hz, ride quality has the same value for rigid and flexible car body.

Parametric Study

The parametric analysis is carried out on the developed dynamically coupled numerical model to study the dynamic behaviour and performance of existing steel–concrete composite railway bridges. The various parameters, i.e. train speed, bridge span length and track properties that affect the dynamic response of the train–track–bridge system, are discussed elaborately in the present work. As mentioned in Sect. 2.1, the ten identical LHB coaches travelling at a constant speed over the simply supported composite bridge are considered for the parametric analysis. As discussed in Sect. 2.2, composite railway bridges of short (19.40 m), medium (25.280 m) and long (31.90 m) span lengths are considered for the parametric study and their equivalent mechanical properties are reported

Table 3 Bridge and rail mechanical properties

S. no	Parameters	Value
A	Bridge	
1	Young's modulus	31.6 GPa
2	Mass density	2750 kg/m^3
3	Poisson's ratio	0.2
4	Damping	2%
5	Span length (L')	19.40 m
5.1	Second moment of area	1.198 m^4
5.2	Cross-sectional area	2.55 m^2
5.3	Mass/length	6498 kg/m
5.4	(D_s) and (D_G)	1.030 m and 1.415 m
6	Span length (L')	25.280 m
6.1	Second moment of area	2.436 m^4
6.2	Cross-sectional area	2.94 m^2
6.3	Mass/length	7492 kg/m
6.4	(D_s) and (D_G)	1.030 m and 1.887 m
7	Span length (L')	31.90 m
7.1	Second moment of area	4.932 m^4
7.2	Cross-sectional area	3.47 m^2
7.3	Mass/length	8843 kg/m
7.4	(D_s) and (D_G)	1.030 m and 2.558 m
B	Rail	
1	Young's modulus	210 GPa
2	Mass density	7850 kg/m^3
3	Cross-sectional area	1.218 m^2
4	Second moment of area	3.217×10^{-5} m^4

Table 4 Properties of ballasted track structure

| S. no	Remarks	Equivalent stiffness (MN/m)	Equivalent damping (kN s/m)
1	R1	64	25
2	R2	94	30
3	R3	112	32
4	R4	124	35
5	R5	132	37
6	R6	138	39

in Table 3. The properties of the ballasted track structure currently in use in the Indian Railways calculated using the spring analogy are elaborated in Table 4. The overall stiffness and damping of ballasted track structure increase from R1 to R6.

Dynamic Behaviour of Train–Track–Bridge System

The bridge responses are evaluated at different speeds ranging from 2 m/s (7.2 km/h) to 110 m/s (396 km/h) for varying track properties and various span lengths to study the dynamic behaviour of the bridge structures under the influence of LHB trains. The maximum displacement and acceleration obtained at the midpoint of a bridge using a validated numerical model at different speeds for various span lengths are shown in Fig. 8. The displacement and acceleration increase with an increase in train speed and reaches a peak value at a bridge's resonance speed for all the span lengths. Further, with an increase in span length, bridges' flexural rigidity and stiffness increase, leading to a decrease in acceleration amplitude, as shown in Fig. 8. It is also interesting that, except at higher speeds where amplitude somewhat fluctuates with a change in track parameters, the influence of track stiffness and damping on bridge response is insignificant.

The resonance property is an essential natural characteristic that governs the bridge design [43]. The train loading mainly excites two types of frequencies in the bridge structures, i.e. driving and dominant frequencies. Driving frequencies [79] depend on the vehicle's duration of crossing the bridge, and dominant frequencies [80] arise due to repeated loads. Mathematically, driving frequencies (f_{dr}) can be represented as, $f_{dr} = nv/2L'$ and dominant frequencies (f_{do}) can be represented as, $f_{do} = nv/L_c$ [81] where L_c denotes the characteristic length of a vehicle compartment (24 m), v is the train speed in m/s, and $n = 1, 2, 3, \ldots, \infty$ represents a higher harmonic frequency. The driving frequencies are contained in the bridge dynamic response due to a single moving vehicle, and when these frequencies approach the bridge fundamental frequency, amplification

Fig. 8 Bridge midpoint displacement for span length of **a** 19.4 m, **c** 25.28 m, **e** 31.9 m and bridge midpoint acceleration for span length of **b** 19.4 m, **d** 25.28 m, **f** 31.9 m
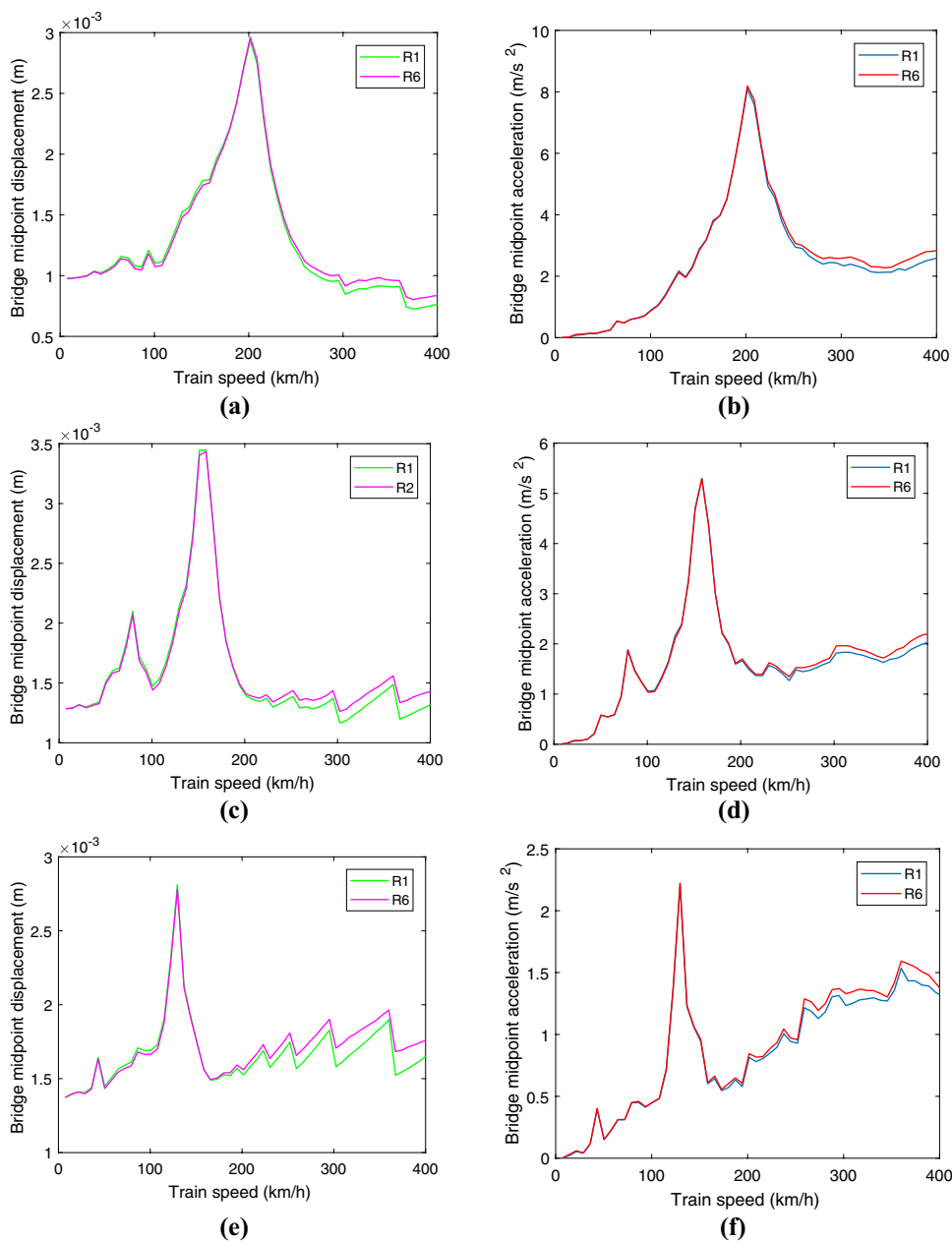
in the bridge response occurs, giving rise to the critical speed. The current study focuses on the dynamic behaviour of railway bridges associated with repeated loads induced by multiple cars passing through. These repeated loads give rise to dominant frequencies. When a dominant frequency or its integral multiple approaches the bridge fundamental frequency, the bridge response is amplified.

The speed parameter S_k, defined as the ratio of the exciting frequency to the frequency of the beam is another critical factor considered in bridge dynamics and is represented using the following expression,

$$S_k = \frac{k\pi v}{\omega_k L'}, \tag{13}$$

here ω_k is the kth natural frequency of the simply supported bridge structure. The speed parameter S_1 of the first mode [82] primarily governs the maximum dynamic response of the beam travelled by the vehicle. Further, Yang et al. [83] showed that for the given compartment length and span length, the resonant speed parameter could be found as;

$$S_1 = \frac{L_c}{2nL'}. \tag{14}$$

Fig. 9 Comparison of bridge midpoint displacement and frequency spectrum for span length of **a**, **b** 19.4 m; **c**, **d** 25.28 m; **e**, **f** 31.9 m
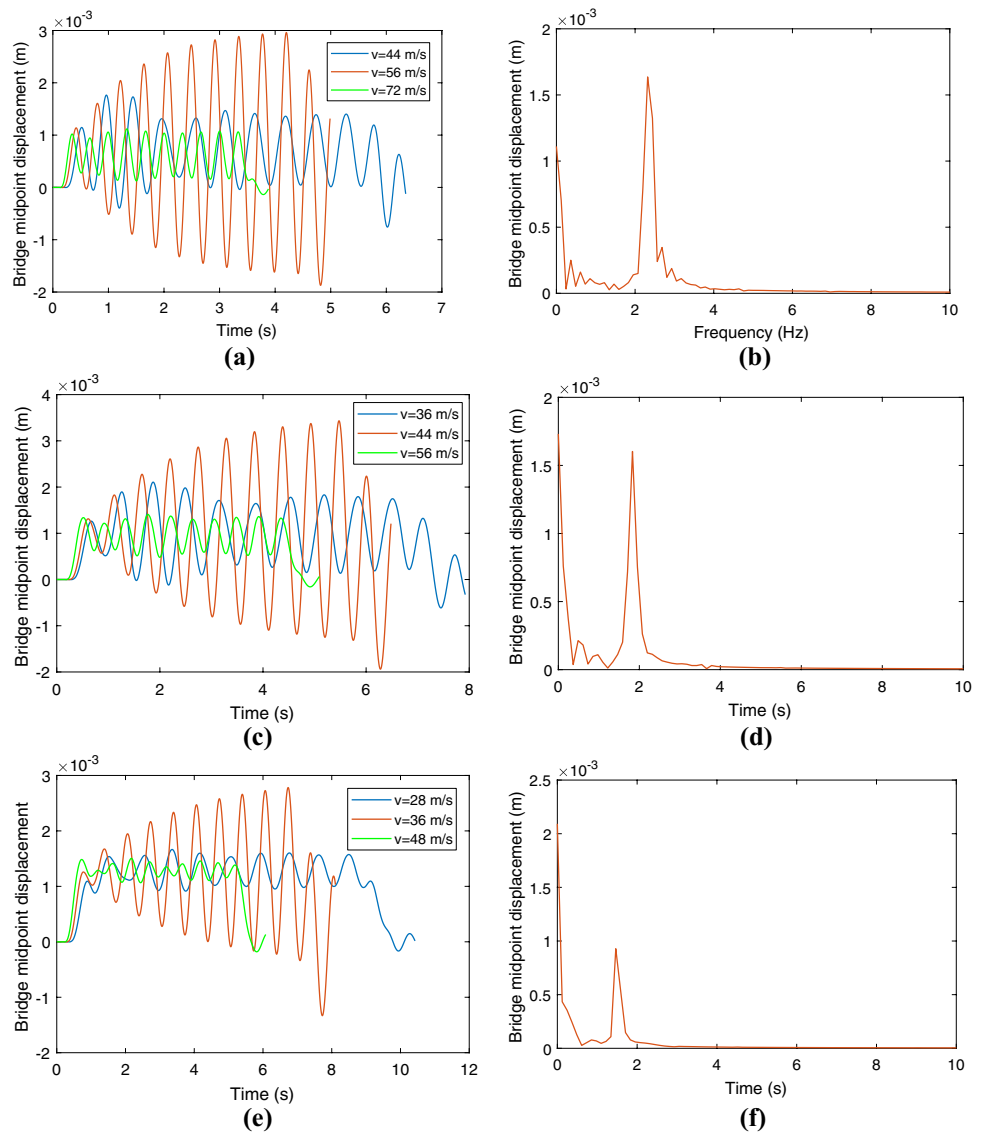

Table 5 Critical frequencies

S. no	Span length (m)	Resonance speed (m/s)	Fundamental frequency of the bridge (Hz)	Dominant frequency (Hz) $n = 4$	$S_1 = \frac{v}{2f_1 L'}$	$S_1 = \frac{L_c}{2nL'}$
1	19.40	56	9.38	9.33	0.154	0.154
2	25.28	44	7.335	7.33	0.119	0.119
3	31.90	36	6.034	6	0.094	0.094

The resonance may occur at $S_1 = 0.50L_c/L', 0.250\ \ L_c/L',$ $S_1 = 0.50L_c/L', 0.250\ \ L_c/L', 0.167\ \ L_c/L', 0.125\ \ L_c/L', \ldots$ by letting $n = 1, 2, 3, \ldots, \infty$ in Eq. (14). The time and frequency domain comparisons of midpoint displacement of the bridge of various span lengths are shown in Fig. 9, and the critical frequencies are shown in Table 5.

The resonance takes place when the integral multiple of the dominant frequency f_{do} matches the fundamental frequency of the bridge. Moreover, as seen in Table 5, the speed parameter S_1 obtained from Eq. (13) satisfies Eq. (14) for $n = 4$ at resonance condition. Further, the frequency plot shown in Fig. 9b, d and f shows enlarged peaks of dominant frequencies. Moreover, at resonance speed, as seen from Fig. 9a, c and e, a clear amplification can be seen in

the bridge's midpoint response; however, bridge deflection closely resembles the trainload pattern at all other speeds.

Dynamic Impact Factor of Bridges

The dynamic effect of a running train is higher in bridge members than normal static load, and this effect is considered in the bridge design codes as an impact factor (I) [84]. The impact factor depends on several factors, including bridges' and vehicles' dynamic characteristics and actions [85]. Mathematically, the impact factor is represented by the following expression,

$$I = \frac{d_{dyn} - d_{sta}}{d_{sta}}, \tag{15}$$

here d_{dyn} and d_{sta} are the maximum dynamic and static displacement of the midpoint of a bridge evaluated at different speeds, respectively. In most design codes, span length is identified as a critical factor affecting the dynamic response of a bridge structure and is an essential parameter of bridge design. Numerous design codes evaluate impact factors in terms of span length; for instance, RDSO [86] suggests Eq. (16) to consider the impact factor of a single span track subjected to a maximum speed of 160 kmph (44.4 m/s);

$$I = 0.15 + \frac{8}{6 + L}. \tag{16}$$

AASTHO manual recommends Eq. (17) for impact factor;

$$I = \frac{15.24}{L + 38.1} < 30\%. \tag{17}$$

Iranian code suggests Eq. (18) for evaluating impact factor;

$$I = \begin{cases} \frac{1.44}{\sqrt{L}-0.2} + 0.82 : \text{Good maintenance} \\ \\ \frac{2.16}{\sqrt{L}-0.2} + 0.73 : \text{Other situations} \end{cases}. \tag{18}$$

The American Railway Engineering and Maintenance-of-Way Association (AREMA) has proposed Eq. (19) for calculating the impact factor in steel railway bridges;

Table 6 Bridge impact factor

S. no	Span length (m)	RDSO	AASTHO	Iranian code	AREMA
1	19.4	0.46	0.26	0.30	0.32
2	25.28	0.41	0.24	0.15	0.27
3	31.9	0.36	0.22	0.1	0.24

Fig. 10 Bridge impact factor for span length of **a** 19.4 m, **b** 25.28 m, **c** 31.9 m
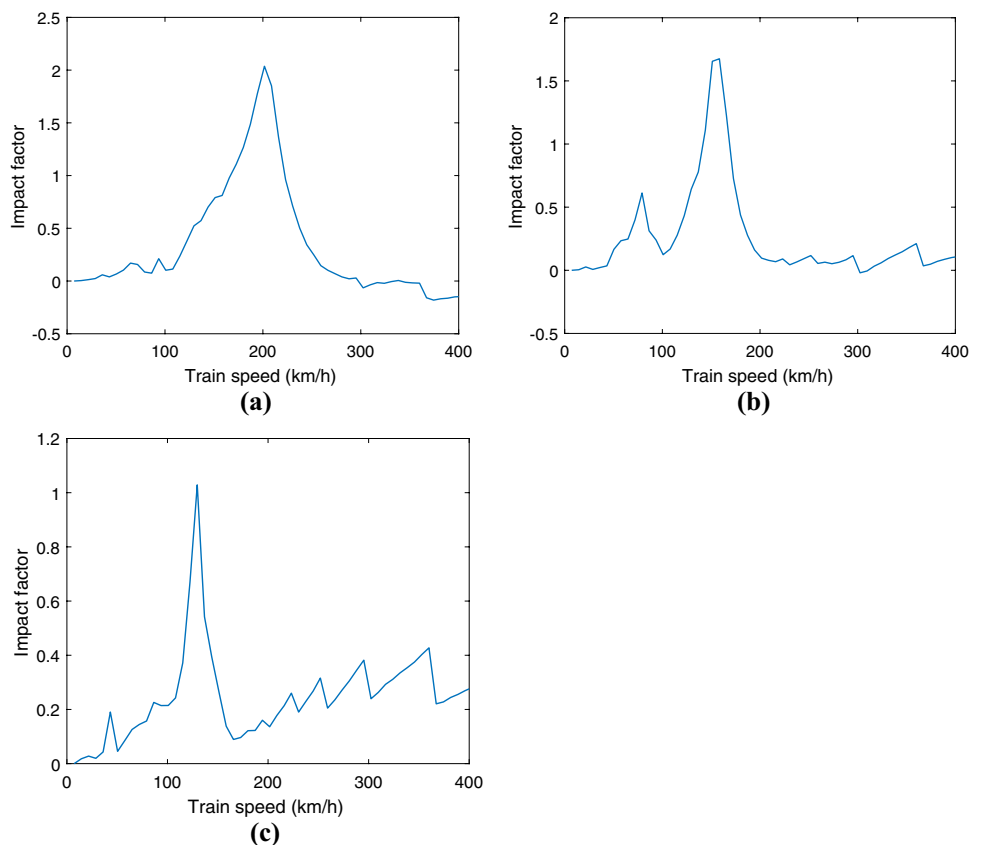
$$I = \begin{cases} 40 - \frac{3L^2}{148.6} & L \le 24 \\ 16 + \frac{182.9}{L-9.1} & L \ge 24 \end{cases}. \qquad (19)$$

The bridge impact factors obtained from the validated model are shown in Fig. 10, and the comparison of impact factors of different standards is given in Table 6.

It can be seen that the impact factor of the bridge is below the limitation set by different standards except at the resonance condition. Further, it can be observed that the impact factor decreases with an increase in span length. Moreover, multiple or single-tuned mass dampers can be used to counter the effect of resonance in composite bridges [87, 88].

Table 7 Classification and vibration limits [89]

S. no	Application scope	For night time (dB)	For day time (dB)
1	Special residential areas	65	65
2	Residential and cultural educational areas	67	70
3	Central business district	72	75
4	Industrial area	72	75
5	Arterial road surrounding	72	75
6	Railway trunk surrounding	80	80

However, the application of tuned mass dampers is beyond the scope of the present study.

Environmental Impact of High-Speed Train

Several standards are available worldwide to evaluate and supervise the vibrations generated inside a structure due to railways. As discussed in the International standard ISO 2631-1-1997 [27], the frequency weighting technique is adopted to evaluate the vertical vibration acceleration level (VAL) in decibel (dB). The evaluated vibration levels are compared with the Chinese standard GB 10070-88 [89] limits listed in Table 7 for various application scopes.

The vibration levels are evaluated using the acceleration responses generated on the bridge structure. The vibration levels produced near railway lines or inside the structures near the high-speed corridors are assumed to be comparable to a vibration level generated at the bridge structure [57]. The VAL for the long-span bridge is relatively lower in magnitude than short and medium-span bridges, as seen in Fig. 11. In addition, in general, a steep rise can be seen in VAL until resonance occurs, and after that, a gradual increase is observed. Moreover, the VAL for all the span lengths surpasses the threshold limit of 80 dB mentioned in Table 7, which may cause damage to the nearby structures and affect human comfort. Besides this, obtained vibration levels are compared with the vibration level criteria curve

Fig. 11 Vibration level for span length of **a** 19.4 m, **b** 25.28 m, **c** 31.9 m. **d** Vibration level criteria curve for detailed vibration analysis
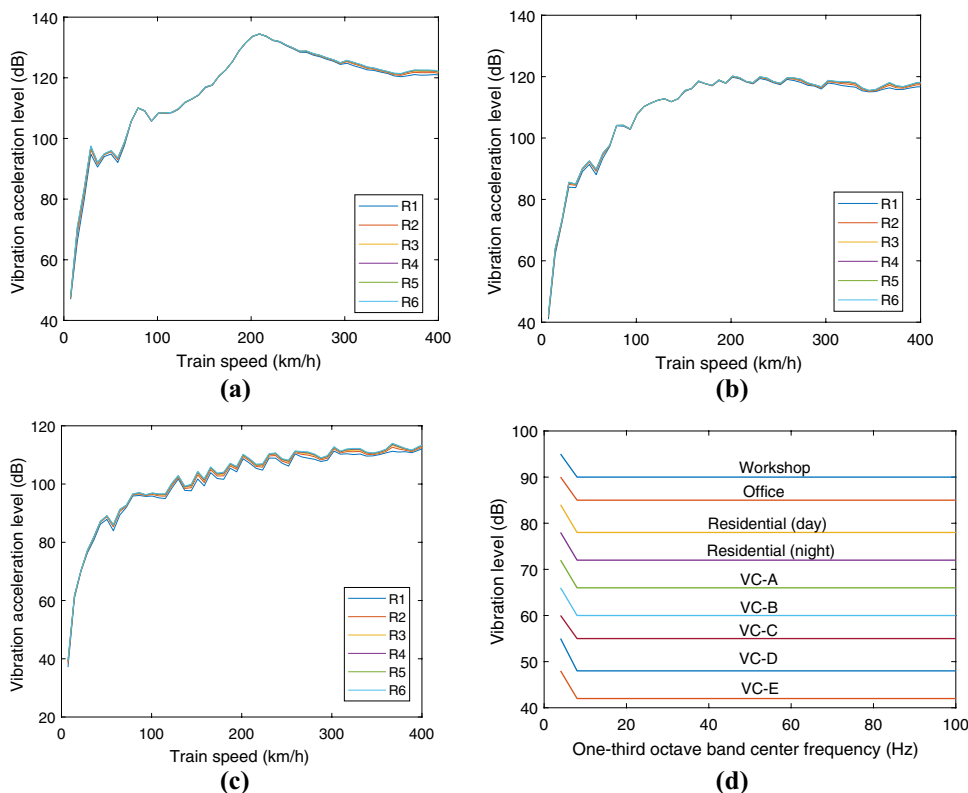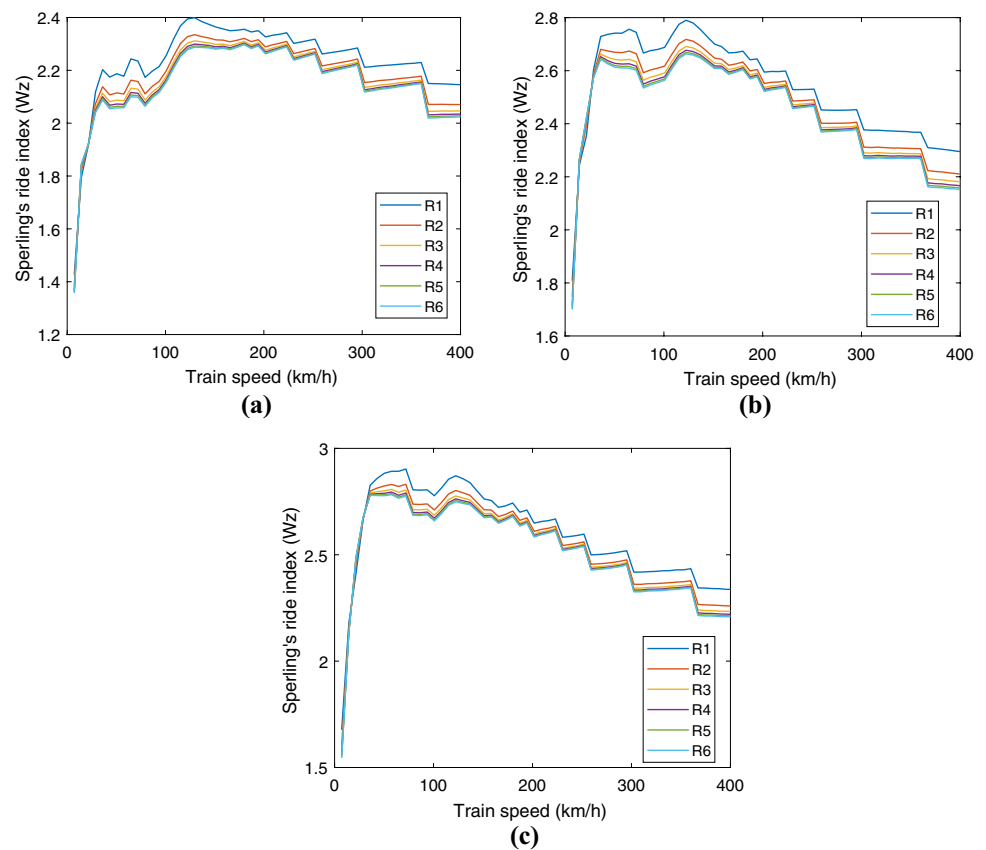
Fig. 12 Sperling's Ride Index for span length of **a** 19.4 m, **b** 25.28 m, **c** 31.9 m

of FTA [36] shown in Fig. 11d, and it can be seen that the vibration level surpasses the limit for each type of land use. Thus it becomes imperative to adopt vibration mitigation measures [35] on or near the track to reduce train-induced vibrations' adverse effects.

Ride Comfort of LHB Coaches

The ride comfort of vehicles is of great concern for the trains travelling at high speed on the bridges [90]. In the present analysis, the SI explained in Sect. 4 is calculated at various speeds and track properties for short, medium, and long-span bridges to assess the ride comfort of the vehicles. The SI evaluated for different conditions is shown in Fig. 12, and it is clear that ride comfort varies considerably with the span length and track properties. For all the span lengths, a steep rise in ride index value can be seen upto 40 kmph, and after that, a gradual decline can be seen with an increase in the train speed.

Moreover, it can be seen that the train's ride comfort surpasses the threshold value ($Wz = 2.5$) at a very low speed for medium and long-span railway bridges, but for small-span bridges ride index lies well below the threshold value, owing to the fact that low frequencies generated in medium and long-span bridges amplify the train vibration modes. Furthermore, a general observation is that ride comfort

improves with an increase in track damping and stiffness at the same speed.

Conclusions

The present work investigated the efficiency of existing steel–concrete composite railway bridges subjected to a high-speed train. A coupled approach based on the two-dimensional finite element method has been used to develop the train–track–bridge dynamic interaction model. The generalised research has been carried out using the case study of Indian Railways. The dynamic performance of the existing composite girder railway bridge is adequate to operate the high-speed train; however, the critical assessment of the railway bridge is necessary under resonance conditions. The ride comfort estimated using Sperling's ride index has shown significant variation with span length and is "clearly noticeable" at medium and high speeds for all span lengths. Moreover, the vibration level generated due to high-speed trains has exceeded the limitations set by FTA and GB 10070-88 for various land use categories. This might annoy residents and cause minor damage to nearby structures unless some mitigation measures are used. In addition, research highlights that increasing the stiffness and damping of the track from R1 to R6 has no considerable effect on the

bridge response. However, ride comfort has improved with an increase in track damping and stiffness at the same speed.

It is worth noting that although some assumptions related to the modelling of bridges and trains have limited the application of the proposed model, the presented approach has effectively simplified the calculation of the complex interaction of the train–track–bridge system.

Declarations

Conflict of interest The authors declare that there is no conflict of interest regarding the publication of this paper. No funding was received for conducting this study.

References

1. Grubisic V, Zagheni E, Asaff Y, Dias A (2015) A framework for categorizing risks in high speed train (HST) projects: the example of the first HST in Brazil. Transp Probl 10:37–46. https://doi.org/10.21307/tp-2015-060

2. NHSRCL. National high speed rail corporation limited 2019. https://nhsrcl.in/index.php/en/project/project-highlights. Accessed 29 Dec 2019.

3. Montenegro PA, Carvalho H, Ribeiro D, Calçada R, Tokunaga M, Tanabe M et al (2021) Assessment of train running safety on bridges: a literature review. Eng Struct 241:112425. https://doi.org/10.1016/j.engstruct.2021.112425

4. Zhai W, Han Z, Chen Z, Ling L, Zhu S (2019) Train–track–bridge dynamic interaction: a state-of-the-art review. Veh Syst Dyn 57:984–1027. https://doi.org/10.1080/00423114.2019.1605085

5. Zeng ZP, Yu ZW, Zhao YG, Xu WT, Chen LK, Lou P (2014) Numerical simulation of vertical random vibration of train-slab track–bridge interaction system by PEM. Shock Vib 2014:1–21. https://doi.org/10.1155/2014/304219

6. Guo W, Wang Y, Liu H, Long Y, Jiang L, Yu Z (2021) Running safety assessment of trains on bridges under earthquakes based on spectral intensity theory. Int J Struct Stab Dyn. https://doi.org/10.1142/S0219455421400083

7. Liu K, Reynders E, De Roeck G, Lombaert G (2009) Experimental and numerical analysis of a composite bridge for high-speed trains. J Sound Vib 320:201–220. https://doi.org/10.1016/j.jsv.2008.07.010

8. Mao L, Lu Y (2013) Critical speed and resonance criteria of railway bridge response to moving trains. J Bridg Eng 18:131–141. https://doi.org/10.1061/(asce)be.1943-5592.0000336

9. Eroğlu M, Koç MA, Esen İ, Kozan R (2022) Train–structure interaction for high-speed trains using a full 3D train model. J Braz Soc Mech Sci Eng. https://doi.org/10.1007/s40430-021-03338-1

10. Chellini G, Nardini L, Salvatore W (2011) Dynamical identification and modelling of steel-concrete composite high-speed railway

11. Liu K, Zhou H, Shi G, Wang YQ, Shi YJ, De Roeck G (2013) Fatigue assessment of a composite railway bridge for high speed trains. Part II: conditions for which a dynamic analysis is needed. J Constr Steel Res 82:246–254. https://doi.org/10.1016/j.jcsr.2012.11.014

12. Adam C, Heuer R, Ziegler F (2012) Reliable dynamic analysis of an uncertain compound bridge under traffic loads. Acta Mech 223:1567–1581. https://doi.org/10.1007/s00707-012-0641-0

13. Nguyen K, Velarde C, Goicolea JM (2019) Analytical and simplified models for dynamic analysis of short skew bridges under moving loads. Adv Struct Eng 22:2076–2088. https://doi.org/10.1177/1369433219831481

14. Hoorpah W (2008) Dynamic calculations of high-speed railway bridges in France-some case studies. Dyn High Speed Railw Bridge. https://doi.org/10.1201/9780203895405.ch9

15. Sieffert Y, Michel G, Ramondenc P, Jullien J-F (2006) Effects of the diaphragm at midspan on static and dynamic behaviour of composite railway bridge: a case study. Eng Struct 28:1543–1554. https://doi.org/10.1016/j.engstruct.2006.02.011

16. Ticona Melo LR, Malveiro J, Ribeiro D, Calçada R, Bittencourt T (2020) Dynamic analysis of the train-bridge system considering the non-linear behaviour of the track–deck interface. Eng Struct 220:110980. https://doi.org/10.1016/j.engstruct.2020.110980

17. Matsuoka K, Collina A, Sogabe M (2017) Dynamic simulation and critical assessment of a composite bridge in high-speed railway. Procedia Eng 199:3027–3032. https://doi.org/10.1016/j.proeng.2017.09.405

18. Shibeshi RD, Roth CP (2016) Field measurement and dynamic analysis of a steel truss railway bridge. S Afr Inst Civ Eng 58:28–36. https://doi.org/10.17159/2309-8775/2016/v58n3a4

19. Arvidsson T, Karoumi R (2014) Train–bridge interaction—a review and discussion of key model parameters. Int J Rail Transp 2:147–186. https://doi.org/10.1080/23248378.2014.897790

20. Zhu Z, Wang L, Costa PA, Bai Y, Yu Z (2019) An efficient approach for prediction of subway train-induced ground vibrations considering random track unevenness. J Sound Vib 455:359–379. https://doi.org/10.1016/j.jsv.2019.05.031

21. Xia H, Li HL, Guo WW, De Roeck G (2014) Vibration resonance and cancellation of simply supported bridges under moving train loads. J Eng Mech 140:1–11. https://doi.org/10.1061/(asce)em.1943-7889.0000714

22. Xia H, Zhang N, Guo WW (2006) Analysis of resonance mechanism and conditions of train-bridge system. J Sound Vib 297:810–822. https://doi.org/10.1016/j.jsv.2006.04.022

23. Zheng L, Jiang L, Feng Y, Liu X, Lai Z, Zhou W (2020) Effects of foundation settlement on comfort of riding on high-speed train–track–bridge coupled systems. Mech Based Des Struct Mach. https://doi.org/10.1080/15397734.2020.1784204

24. Kargarnovin MH, Younesian D, Thompson D, Jones C (2005) Ride comfort of high-speed trains travelling over railway bridges. Veh Syst Dyn 43:173–197. https://doi.org/10.1080/00423110512331335111

25. Arvidsson T, Andersson A, Karoumi R (2019) Train running safety on non-ballasted bridges. Int J Rail Transp 7:1–22. https://doi.org/10.1080/23248378.2018.1503975

26. Jiang Y, Chen BK, Thompson C (2019) A comparison study of ride comfort indices between Sperling's method and EN 12299. Int J Rail Transp 7:279–296. https://doi.org/10.1080/23248378.2019.1616329

27. ISO (1997) ISO 2631-1-1997: mechanical vibration and shock—evaluation of human exposure to whole-body vibration—part 1: General Requirements, vol 1997

28. Montenegro PA, Ribeiro D, Ortega M, Millanes F, Goicolea JM, Zhai W et al (2022) Impact of the train–track–bridge system

characteristics in the runnability of high-speed trains against crosswinds - Part II: riding comfort. J Wind Eng Ind Aerodyn 224:104987. https://doi.org/10.1016/j.jweia.2022.104987

29. Givoni M (2006) Development and impact of the modern high-speed train: a review. Transp Rev 26:593–611. https://doi.org/10.1080/01441640600589319

30. Avillez J, Frost M, Cawser S, Skinner C, El-Hamalawi A, Shields P (2012) Procedures for estimating environmental impact from railway induced vibration: a review. ASME 2012 Noise Control Acoust. Div. Conf., American Society of Mechanical Engineers; 2012, pp 381–92. https://doi.org/10.1115/NCAD2012-1083

31. Sanayei M, Maurya P, Moore JA (2013) Measurement of building foundation and ground-borne vibrations due to surface trains and subways. Eng Struct 53:102–111. https://doi.org/10.1016/j.engstruct.2013.03.038

32. Kouroussis G, Verlinden O, Conti C (2012) Influence of some vehicle and track parameters on the environmental vibrations induced by railway traffic. Veh Syst Dyn 50:619–639. https://doi.org/10.1080/00423114.2011.610897

33. Li GQ, Wang ZL, Chen S, Xu YL (2016) Field measurements and analyses of environmental vibrations induced by high-speed Maglev. Sci Total Environ 568:1295–1307. https://doi.org/10.1016/j.scitotenv.2016.01.212

34. Cao Z, Xu Y, Gong W, Cai Y, Yuan Z (2020) Probabilistic analysis of environmental vibrations induced by high-speed trains. Soil Dyn Earthq Eng 139:1–5. https://doi.org/10.1016/j.soildyn.2020.106343

35. Kedia NK, Kumar A (2019) A review on vibration generation due to subway train and mitigation techniques. In: Sundaram R, Shahu JT, Havanagi V (eds) Geotechnical transportation infrastructure, vol 28. Springer, Singapore, pp 295–308

36. Quagliata A, Ahearn M, Boeker E, Roof C, Meister L, Singleton H (2018) Transit noise and vibration impact assessment manual. Cambridge

37. Fang M, Cerdas SF (2015) Theoretical analysis on ground vibration attenuation using sub-track asphalt layer in high-speed rails. J Mod Transp 23:214–219. https://doi.org/10.1007/s40534-015-0081-3

38. Zhai W, Sun X (1994) A detailed model for investigating vertical interaction between railway vehicle and track. Veh Syst Dyn 23:603–615. https://doi.org/10.1080/00423119308969544

39. Lee YS, Kim SH, Jung J (2005) Three-dimensional finite element analysis model of high-speed train–track–bridge dynamic interactions. Adv Struct Eng 8:513–528. https://doi.org/10.1260/136943305774858034

40. Lei X (2017) High speed railway track dynamics. Springer, Singapore. https://doi.org/10.1007/978-981-10-2039-1

41. Gu Q, Liu Y, Guo W, Li W, Yu Z, Jiang L (2019) A practical wheel–rail interaction element for modeling vehicle–track–bridge systems. Int J Struct Stab Dyn 19:1–27. https://doi.org/10.1142/S0219455419500111

42. Ouyang H (2011) Moving-load dynamic problems: a tutorial (with a brief overview). Mech Syst Signal Process 25:2039–2060. https://doi.org/10.1016/j.ymssp.2010.12.010

43. Liu K, De Roeck G, Lombaert G (2009) The effect of dynamic train–bridge interaction on the bridge response during a train passage. J Sound Vib 325:240–251. https://doi.org/10.1016/j.jsv.2009.03.021

44. Cheng YS, Au FTK, Cheung YK (2001) Vibration of railway bridges under a moving train by using bridge–track–vehicle element. Eng Struct 23:1597–1606. https://doi.org/10.1016/S0141-0296(01)00058-X

45. Cantero D, Arvidsson T, Obrien E, Karoumi R (2016) Train–track–bridge modelling and review of parameters. Struct Infrastruct Eng 12:1051–1064. https://doi.org/10.1080/15732479.2015.1076854

46. Mu D, Choi D-H (2014) Dynamic responses of a continuous beam railway bridge under moving high speed train with random track irregularity. Int J Steel Struct 14:797–810. https://doi.org/10.1007/s13296-014-1211-1

47. Ozdagli AI, Gomez JA, Moreu F (2017) Real-time reference-free displacement of railroad bridges during train-crossing events. J Bridge Eng 22:04017073. https://doi.org/10.1061/(asce)be.1943-5592.0001113

48. Koh CG, Ong JSY, Chua DKH, Feng J (2003) Moving element method for train-track dynamics. Int J Numer Methods Eng 56:1549–1567. https://doi.org/10.1002/nme.624

49. Zhai W, Cai Z (1997) Dynamic interaction between a lumped mass vehicle and a discretely supported continuous rail track. Comput Struct 63:987–997. https://doi.org/10.1016/S0045-7949(96)00401-4

50. Singh SD, Mathur R, Srivastava RK (2019) Optimization of dynamically sensitive parameters of Linke Hofmann Busch coach considering suspended equipment using design of experiment. JVC Journal Vib Control 25:1793–1811. https://doi.org/10.1177/1077546319832720

51. Suresh BS, Prithvi C, Ramachandracharya S (2020) Modal analysis of FIAT Bogie of LHB railway coach. Mater Today Proc 27:1889–1893. https://doi.org/10.1016/j.matpr.2020.03.817

52. Askarinejad H, Dhanasekar M (2016) A multi-body dynamic model for analysis of localized track responses in vicinity of rail discontinuities. Int J Struct Stab Dyn 16:1–33. https://doi.org/10.1142/S0219455415500583

53. Zhai W, Wang K, Cai C (2009) Fundamentals of vehicle–track coupled dynamics. Veh Syst Dyn 47:1349–1376. https://doi.org/10.1080/00423110802621561

54. Salcher P, Adam C, Kuisle A (2019) A stochastic view on the effect of random rail irregularities on railway bridge vibrations. Struct Infrastruct Eng 15:1649–1664. https://doi.org/10.1080/15732479.2019.1640748

55. Yang YB, Yau JD, Wu YS (2004) Vehicle–bridge interaction dynamics. World Scientific, Singapore. https://doi.org/10.1142/5541

56. Sun YQ, Cole C, Spiryagin M, Dhanasekar M (2013) Vertical dynamic interaction of trains and rail steel bridges. Electron J Struct Eng 13:88–97

57. Kedia NK, Kumar A, Singh Y (2021) Effect of rail irregularities and rail pad on track vibration and noise. KSCE J Civ Eng 25:1341–1352. https://doi.org/10.1007/s12205-021-1345-6

58. Lei X, Noda N-A (2002) Analyses of dynamic response of vehicle and track coupling system with random irregularity of track vertical profile. J Sound Vib 258:147–165. https://doi.org/10.1006/jsvi.2002.5107

59. Xia H, Zhang N, Guo W (2018) Dynamic interaction of train-bridge systems in high-speed railways. Springer, Berlin. https://doi.org/10.1007/978-3-662-54871-4

60. Eurocode-Basis of Structural Design EN 1990:2002+A1:2005 (2010). vol 1. Brussels

61. Antolín P, Zhang N, Goicolea JM, Xia H, Astiz MÁ, Oliva J (2013) Consideration of nonlinear wheel–rail contact forces for dynamic vehicle–bridge interaction in high-speed railways. J Sound Vib 332:1231–1251. https://doi.org/10.1016/j.jsv.2012.10.022

62. Bathe KJ (2014) Finite element procedures, 2nd edn. K. J Bathe, Watertown

63. Xu YL, Zhang N, Xia H (2004) Vibration of coupled train and cable-stayed bridge systems in cross winds. Eng Struct 26:1389–1406. https://doi.org/10.1016/j.engstruct.2004.05.005

64. Zhang N, Xia H (2013) Dynamic analysis of coupled vehicle–bridge system based on inter-system iteration method. Comput

Struct 114–115:26–34. https://doi.org/10.1016/j.compstruc.2012.10.007

65. Yang F, Fonder GA (1996) An iterative solution method for dynamic response of bridge-vehicles systems. Earthq Eng Struct Dyn 25:195–215

66. Lou P, Zeng Q (2005) Formulation of equations of motion of finite element form for vehicle–track–bridge interaction system with two types of vehicle model. Int J Numer Methods Eng 62:435–474. https://doi.org/10.1002/nme.1207

67. Lou P (2007) Finite element analysis for train–track–bridge interaction system. Arch Appl Mech 77:707–728. https://doi.org/10.1007/s00419-007-0122-4

68. Heckl M, Hauck G, Wettschureck R (1996) Structure-borne sound and vibration from rail traffic. J Sound Vib 193:175–184. https://doi.org/10.1006/jsvi.1996.0257

69. Sheng X, Jones CJC, Thompson DJ (2003) A comparison of a theoretical model for quasi-statically and dynamically induced environmental vibration from trains with measurements. J Sound Vib 267:621–635. https://doi.org/10.1016/S0022-460X(03)00728-4

70. Au FTK, Wang JJ, Cheung YK (2002) Impact study of cable-stayed railway bridges with random rail irregularities. Eng Struct 24:529–541. https://doi.org/10.1016/S0141-0296(01)00119-5

71. Podwórna M (2015) Modelling of random vertical irregularities of railway tracks. Int J Appl Mech Eng 20:647–655. https://doi.org/10.1515/ijame-2015-0043

72. Sadeghi J, Rabiee S, Khajehdezfuly A (2019) Effect of rail irregularities on ride comfort of train moving over ballast-less tracks. Int J Struct Stab Dyn 19:1–28. https://doi.org/10.1142/S0219455419500603

73. ORE Reports C116/RP 1-9/EC 1971-1978 (1978) Interaction between vehicle and track. Utrecht

74. Bokaeian V, Rezvani MA, Arcos R (2019) The coupled effects of bending and torsional flexural modes of a high-speed train car body on its vertical ride quality. Proc Inst Mech Eng Part K J Multi Body Dyn 233:979–993. https://doi.org/10.1177/1464419319856191

75. Wang K, Xia H, Xu M, Guo W (2015) Dynamic analysis of train–bridge interaction system with flexible car-body. J Mech Sci Technol 29:3571–3580. https://doi.org/10.1007/s12206-015-0801-y

76. Dumitriu M, Dihoru II (2021) Influence of bending vibration on the vertical vibration behaviour of railway vehicles carbody. Appl Sci 11:8502. https://doi.org/10.3390/app11188502

77. Dumitriu M, Cruceanu CǍ (2017) Influences of carbody vertical flexibility on ride comfort of railway vehicles. Arch Mech Eng 64:221–238. https://doi.org/10.1515/meceng-2017-0014

78. Zhou J, Goodall R, Ren L, Zhang H (2009) Influences of car body vertical flexibility on ride quality of passenger railway vehicles. Proc Inst Mech Eng Part F J Rail Rapid Transit 223:461–471. https://doi.org/10.1243/09544097JRRT272

79. Yang YB, Lin CW (2005) Vehicle–bridge interaction dynamics and potential applications. J Sound Vib 284:205–226. https://doi.org/10.1016/j.jsv.2004.06.032

80. Ju SH, Lin HT, Huang JY (2009) Dominant frequencies of train-induced vibrations. J Sound Vib 319:247–259. https://doi.org/10.1016/j.jsv.2008.05.029

81. Ju SH, Lin HT (2003) Resonance characteristics of high-speed trains passing simply supported bridges. J Sound Vib 267:1127–1141. https://doi.org/10.1016/S0022-460X(02)01463-3

82. Yang Y-B, Liao S-S, Lin B-H (1995) Impact formulas for vehicles moving over simple and continuous beams. J Struct Eng 121:1644–1650. https://doi.org/10.1061/(ASCE)0733-9445(1995)121:11(1644)

83. Yang YB, Yau JD, Hsu LC (1997) Vibration of simple beams due to trains moving at high speeds. Eng Struct 19:936–944. https://doi.org/10.1016/s0141-0296(97)00001-1

84. Lee HH, Jeon JC, Kyung KS (2012) Determination of a reasonable impact factor for fatigue investigation of simple steel plate girder railway bridges. Eng Struct 36:316–324. https://doi.org/10.1016/j.engstruct.2011.12.021

85. Jung H, Kim G, Oh J, Park J (2019) Design criteria for impact factors based on dynamic on-site data in railway bridges. Struct Infrastruct Eng 15:484–491. https://doi.org/10.1080/15732479.2018.1562476

86. Ministry of Railways I (2014) Bridge rules: rules specifying the loads for design of super-structure and sub-structure of bridges for assessment of the strength of existing bridges, vol 2014. Lucknow

87. Zhou D, Li J, Hansen CH (2013) Suppression of the stationary maglev vehicle-bridge coupled resonance using a tuned mass damper. JVC J Vib Control 19:191–203. https://doi.org/10.1177/1077546311430716

88. Li J, Su M, Fan L (2005) Vibration control of railway bridges under high-speed trains using multiple tuned mass dampers. J Bridge Eng 10:312–320. https://doi.org/10.1061/(ASCE)1084-0702(2005)10:3(312)

89. Standards press of C (1988) GB 10070-88: Standard of vibration in urban area environment. Beijing

90. Youcef K, Sabiha T, El Mostafa D, Ali D, Bachir M (2013) Dynamic analysis of train-bridge system and riding comfort of trains with rail irregularities. J Mech Sci Technol 27:951–962. https://doi.org/10.1007/s12206-013-0206-8